Theoretical and Experimental X-Ray Photoelectron Spectroscopy Investigation of Ion-Implanted Nafion

EUFROZINA A. HOFFMANN,[1,2] ZOLTAN A. FEKETE,[1,2] LJILJANA S. KORUGIC-KARASZ,[1] FRANK E. KARASZ,[1] EUGENE WILUSZ[3]

[1]Department of Polymer Science and Engineering, University of Massachusetts, Amherst, Massachusetts 01003

[2]Department of Physical Chemistry, University of Szeged, Szeged, Hungary H-6701

[3]U.S. Army Natick Soldier Center, Natick, Massachusetts 01760

Received 18 March 2003; accepted 13 June 2003

ABSTRACT: The membrane properties of a Nafion surface can be modified by ion implantation with N^+ or F^+. The results are presented of an X-ray photoelectron spectroscopy (XPS) study of implanted surfaces. For the interpretation of the XPS spectra, calculations using a semiempirical quantum chemical formalism (AM1) have been applied, in conjunction with a charge–potential model, to predict the C_{1s} core electron binding energies. © 2003 Wiley Periodicals, Inc. J Polym Sci Part A: Polym Chem 42: 551–556, 2004

Keywords: semiempirical calculations; quantum chemistry; fluoropolymers; ESCA/XPS; theory

INTRODUCTION

Nafion is a copolymer of tetrafluoroethylene and perfluoro[2-(fluorosulfonylethoxy)-vinyl]ether,[1] and it is widely used in fuel cells as an electrolyte membrane. This polymer has been a subject of interest because of its membrane properties, such as proton transport combined with chemical inertness.[2–16] Ion implantation can further modify the properties by developing barrier layers that are selectively permeable to water vapor.

In the ion-implantation process, the target surface is bombarded by a beam of ions. In this technique, the ion energy is typically 100 keV or more, at normal incidence to the surface; this results in penetration depths of hundreds of nanometers. In contrast, in ion etching, a related technique, the removal of one or more layers of atoms is achieved by ion beams hitting the substrate at nonnormal angles with energies in the range of 1–5 keV. This leads to penetration depths of a few nanometers and the transfer of collisional energy to target atoms.

X-ray photoelectron spectroscopy (XPS) is a widely used method for surface analysis that can be applied to the analysis of polymer materials.[17–19] Although X-ray exposure can damage polymers, this problem becomes significant in perfluorinated polymers only after exposures of over 30 min.[20,21] Insulators pose a problem in this technique because of charge buildup, and so peak positions are usually assigned with respect to a known peak in the spectrum. The assignment of the peaks can be greatly aided by parallel theoretical considerations.

It has been recognized that partial atomic charges play a decisive role in determining the shifts of the binding energy (E_b).[22] Calculated charges have been used to correlate chemical

Journal of Polymer Science: Part A: Polymer Chemistry, Vol. 42, 551–556 (2004)
© 2003 Wiley Periodicals, Inc.

shifts in fluoropolymers.[23] Early calculations applied the CNDO approximation to estimate charges, and this provided good fits within groups of related compounds. However, the fit across different groups was less satisfactory.[23]

Recently, there have been applications of *ab initio* methods to the calculation of C_{1s} core electron binding energies[24–26] for polymers, based ultimately on oligomer models containing a few monomer units. Although such a calculation can, in principle, provide E_b directly, it has been found that an added empirical shift is necessary for the results to agree with experiments. For systems of moderate size, this method provides good results; however, the computational time grows rapidly if the molecules contain many heavier (nonhydrogen) atoms, as is the case for perfluorinated polymers. In contrast, the semiempirical Austin Model 1 (AM1) method yields adequate geometries for large molecules with relatively modest computational effort. Sleigh et al.[27] demonstrated the utility of AM1 calculations for determining partial atomic charges to correlate them with XPS core binding energies for the elements H, C, N, O, and F as well as a number of metals. They did not apply the additional correction related to the Madelung potential (discussed later), and halogenated polymers were excluded from the correlation of C_{1s} binding energies.

Table 1. Experimental Binding Energies (E_b) and Calculated Group Parameters (q_i and $V_{m(i)}$) for Selected Polymers

Abbreviation	Name and Group[a]	q_i (e)	$V_{m(i)}$ (eV)	E_b (eV)[b]	$E_b - V_{m(i)}$ (eV)
PE	Polyethylene $(—C^*H_2—)_n$	−0.158	0.80	285.00	284.20
PMA	Poly(methyl acrylate)				
	$(—CH_2CH[C^*(O)OCH_3]-)_n$	0.294	−5.80	289.04	294.84
	$(—CH_2CH[C(O)OC^*H_3]-)_n$	−0.065	0.81	286.59	285.78
	$(—C^*H_2CH[C(O)OCH_3]-)_n$	−0.103	1.21	285.41	284.20
PMG	Poly(methylene glycol)				
	$(—CH_2C^*H_2O-)_n$	0.109	−2.34	287.89	290.23
PTFE	Poly(tetrafluoroethylene)				
	$(—C^*F_2-)_n$	0.209	−0.40	292.00	292.40
PTFEO–cHFPO	Poly(tetrafluoroethyleneoxide-*co*-hexafluoropropyleneoxide)				
	Fomblin Y				
	$[—OCF(CF_3)CF_2]_n(—OC^*F_2)_m$	0.567	−6.66	294.09	300.75
	$[—OCF(C^*F_3)CF_2]_n(—OCF_2)_m$	0.433	−3.51	293.80	297.31
	$[—OCF(CF_3)C^*F_2]_n(—OCF_2)_m$	0.376	−3.43	293.23	296.66
	$[—OC^*F(CF_3)CF_2]_n(—OCF_2)_m$	0.224	−0.44	291.40	291.84
PTMG	Poly(tetramethylene glycol)				
	$(—CH_2CH_2C^*H_2CH_2O—)_n$	−0.018	−0.89	286.35	287.24
PVA	Poly(vinyl alcohol)				
	$[—CH_2C^*(OH)H—]_n$	0.042	−2.30	286.47	288.77
	$[—C^*H_2C(OH)H—]_n$	−0.197	1.98	285.00	283.02
PVC	Poly(vinyl chloride)				
	$(—C^*HClCH_2—)_n$	−0.064	0.35	287.00	286.65
	$(—CHClC^*H_2—)_n$	−0.176	2.50	285.90	283.40
PVDC	Poly(vinylidene chloride)				
	$(—C^*Cl_2CH_2—)_n$	0.028	−1.05	288.56	289.61
	$(—CCl_2C^*H_2—)_n$	−0.179	3.06	286.16	283.10
PVDF	Poly(vinylidene fluoride)				
	$(—C^*F_2CH_2—)_n$	0.292	−3.98	290.90	294.88
	$(—CF_2C^*H_2—)_n$	−0.261	5.33	286.44	281.11
PVF	Poly(vinyl fluoride)				
	$(—C^*HFCH_2-)_n$	0.061	−1.12	288.00	289.12
	$(—CHFC^*H_2—)_n$	−0.223	3.54	285.90	282.36

[a] An asterisk indicates a specified carbon atom.
[b] Measured XPS binding energy.[17,18]

In this study, we have found that the charge–potential method, combined with AM1 calculations, yields good correlations for a wide variety of polymer structures whose XPS data have been collated in standard databases. This makes it feasible to estimate chemical shifts for various molecular architectures and to guide the peak fitting and resolution of a measured spectrum.

The XPS study of pristine Nafion[21,28] and X-ray degraded and ion-etched Nafion[21] has been reported in the literature. Ion implantation can change Nafion through bond breaking and subsequent rearrangement, and in this calculation, we have monitored this effect by following changes in the chemical shifts. Even though the measuring depth of XPS is much shallower than the total depth achieved in ion implantation, the changes caused by the ion beam are already evident in the XPS interrogated layer,[29,30] and the modification of the chemical structure could be investigated.

EXPERIMENTAL

The substrates used were commercially available Nafion 112 and 117 membranes manufactured by E. I. du Pont de Nemours & Co. (nominal equivalent weight = 1100, thickness = 50 or 175 μm, respectively). Ion implantation was performed in a Whickham 200-keV medium-current ion implanter with total N^+ and F^+ ion fluences of 10^{15} ions/cm^{-2}.

The specimens were stored in a dry nitrogen stream for 2 days to minimize their water content. Further cleaning of the surface was not attempted so that the near-surface structure would be preserved. The samples were mounted on double-sided conductive tape.

The XPS analysis was carried out in a Physical Electronics apparatus with a nonmonochromatic Mg Kα radiation source at a 75° takeoff angle. The sensitivity factors specified for the spectrometer were used for quantitative analysis. The pressure in the analysis chamber was less than 10^{-5} Pa. The spectrum collection time was kept under 10 min to minimize X-ray damage.

The spectra were deconvoluted with standard built-in software by being fit with Gauss–Lorentz peaks (the Gauss–Lorentz ratio was allowed to vary, yielding values of over 0.9 in most cases), as described by Beamson and Briggs,[18] and values of the full width at half-maximum were typically obtained between 2 and 3 eV for resolved peaks.

CALCULATIONS

To interpret the XPS spectra of Nafion and its degradation products, we developed a correlation between the C_{1s} binding energies collated in the literature[17,18] and theoretically derived parameters determined on the basis of their chemical structures. To calculate the structural data and the partial charges, we used the semiempirical quantum chemical formalism AM1, as implemented in the MOPAC program (version 6.0).[31] The geometries were optimized with convergence criteria specified by the keyword *PRECISE*. The optimization was carried out with the eigenvalue-following method. The energies associated with the final geometries were tested to be at a true minimum by the implementation of a normal coordinate analysis and by the determination that all normal frequencies were real. The oligomers used in this calculation contained 7–20 repeating units (ca. 100 atoms). Data for chain ends were not used in the calculations. The partial atomic charges and the coordinates of the molecules at the optimized geometry were taken from the MOPAC output, and the intramolecular Madelung potential of the ith atom ($V_{m(i)}$) was calculated as follows:[22,23]

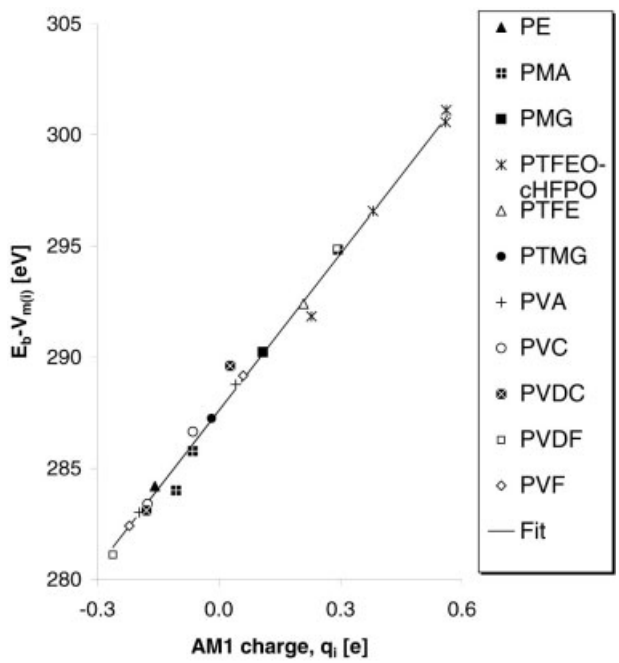

Figure 1. Correlation between $E_b - V_{m(i)}$ and q_i (see Table 1 for the abbreviations).

Table 2. Calculated C_{1s} Binding Energies (eV) in Fragments

	Fragment	Group							
		a	b	c	d	e	f	g	h
1	$^{a}CF_3(^{b}CF_2)_5{}^{c}CF_2{}^{d}C(O)^{c}CF_2(^{b}CF_2)_5{}^{a}CF_3$	293.6	292.1	292.2	291.5				
2	$^{a}CF_3(^{b}CF_2)_7{}^{c}CF_2O^{c}CF_2(^{b}CF_2)_7{}^{a}CF_3$	293.7	292.2	292.7					
3	$^{a}CF_3{}^{b}CF{=}^{c}CF(^{c}CF{=}^{c}CF)_6{}^{c}CF{=}^{b}CF^{a}CF_3$	293.6	288.7	289.2					
4	$CF_3CF_2{}^{b}CF{=}^{b}CF(^{a}CF_2)_3{}^{b}CF{=}^{b}CF$ $(^{a}CF_2)_9{}^{b}CF{=}^{b}CF(^{a}CF_2)_6CF_2CF_3$	292.2	289.0						
5	$(^{a}CF_3(^{b}CF_2)_6)_2{}^{c}CFO^{d}CF_2{}^{e}CF(^{g}CF_3)O^{i}CF{=}^{h}CF_2$	293.6	292.2	291.3	293.3	292.2	289.1	293.6	291.4

$$V_{m(i)} = \sum_{j \neq i} \frac{q_j}{r_{ij}} \quad (1)$$

where j is the index of atoms other than the one whose binding energy is calculated, q_j denotes the charge of the other atoms, and r_{ij} represents the respective distances. Table 1 shows the polymers considered. Representative polymers covering a wide range of C_{1s} binding energies, including the structural moieties of Nafion and its probable fragments, were selected. Sulfur-containing groups were omitted from the calculations because hypervalent sulfur is not validated properly by AM1.[32,33] A plot of the corrected C_{1s} binding energy ($E_b - V_{m(i)}$) versus the calculated partial charge (q_i) of the carbon atoms produces a linear correlation (Fig. 1) with a slope of 23.6 ± 0.4 eV/e, an intercept of 287.6 ± 0.1 eV, and weighted standard error of the estimate of 0.3 eV. The goodness of fit is comparable to the uncertainty of experimental XPS peak positions usually cited as 0.2–0.4 eV[17,18] for nonmonochromatic XPS.

This fit was then used in a calculation predicting the binding energies of C_{1s} in pristine and ion-implanted Nafion. Table 2 shows the data for probable fragments of this polymer.

RESULTS AND DISCUSSION

Figure 2 shows a typical XPS survey spectrum of pristine Nafion 117. In these measurements and others for ion-implanted Nafion, similar spectra were obtained for specimens of different thicknesses. The main constituents (carbon, fluorine, and oxygen) appeared as well-defined peaks, whereas the sulfur yielded a small peak with a poor signal-to-noise ratio. We applied a relative referencing[18,21] correction for the effect of charging, which caused the shifting of the spectra to higher binding energies. The value of the binding energy for carbon in the Teflon-like CF_2 group (292.2 eV) is well known from the literature[17,21] and is in agreement with these calculations. This peak was easily identified in the spectra obtained and was, therefore, used as a reference. The F_{1s} peak was observed at a binding energy of 689.4 eV with an associated satellite peak at 680.8 eV. The O_{1s} peak from the oxygen in the sulfonate group appeared at 532.9 eV, and that of ether oxygen appeared at 535.3 eV.

The C_{1s} signal, shown in detail at the top of Figure 3, was deconvoluted into five peaks, among which CF_2 dominated, with a satellite peak at 281.8 eV. A minor component appeared at 294.4 eV, which was attributed to terminal CF_3 groups. The peak at 289.6 eV was interpreted by comparison with the carbon atom *f* in Table 2 (line 5). The structure of this molecule is very similar to that of Nafion, but it contains a double bond instead of a terminal perfluorethylene group. The effect of this double bond is to lower the binding

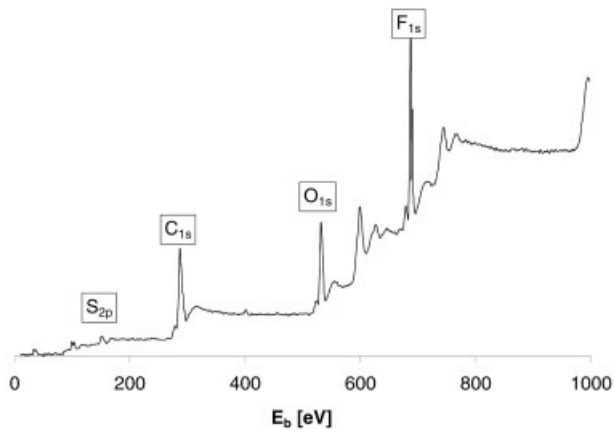

Figure 2. Raw XPS spectrum of Nafion 117.

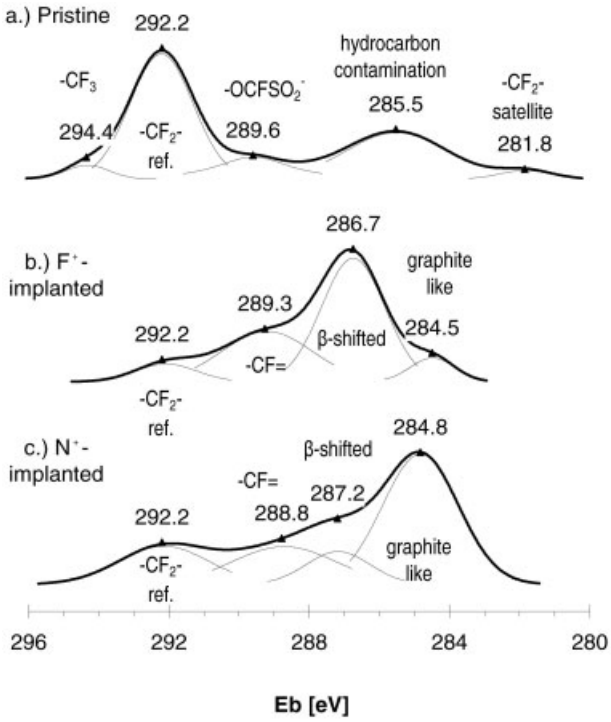

Figure 3. C_{1s} XPS spectra of pristine and implanted Nafion 117.

energy, similarly to the effect of a sulfonate group, which, as already noted, cannot be properly calculated with the AM1 method. The predicted binding energy of 289.1 eV is 0.5 eV lower than the experimental value. It can also be seen from the calculation (Table 2, line 5) that the predicted binding energies of the other carbon atoms with neighboring oxygen are 291.3 (c), 292.2 (e), and 293.3 eV (d). These peaks were not observable beneath the large CF_2 peak, which had a measured full width at half-maximum of 2.7 eV. The peak at 285.6 eV characteristic of hydrocarbons was assumed to originate from surface contamination. This assumption was supported by the fact that the percentage of carbon was higher than expected from the stoichiometry of Nafion. Subtracting the area of this peak brought the carbon/fluorine ratio close to the theoretical value. The relative atomic concentrations calculated on the basis of the theoretical compositions are listed in the first column of Table 3, whereas the measured raw and corrected values are shown in the second and third columns, respectively.

In the ion-implanted Nafion samples, the CF_2 peak was diminished, whereas a number of enhanced peaks appeared at lower binding energies [Fig. 3(b,c)]. In the case of the F^+-implanted Nafion, the lowest binding energy peak corresponded to graphitic carbon (284.5 eV). The peak at 286.7 eV was assigned to carbon in an unsaturated partially fluorinated environment, such as the β-shifted carbon observed by Gould et al.[34] in an XPS spectrum of polydifluoracetylene. There was a component at 289.3 eV corresponding to partially fluorinated carbon, and in light of these calculations for the model fragments, this was likely due to unsaturated moieties, as shown in Table 2 (line 4, atom c). It should be noted that the predicted values of the C_{1s} binding energies in unsaturated groups containing either oxygen or fluorine were very close to one another. In the case of the N^+-implanted samples, the peak positions and amplitudes were slightly changed. There was a graphitic carbon peak at 284.8 eV, a β-shifted carbon at 287.2 eV, and an unsaturated carbon at 288.8 eV (see Table 2, lines 3 and 4, atom b). We observed no significant peaks due to oxygen-bonded carbon in either of the ion-implanted samples. The main difference between the two types of samples was that in the fluorine-implanted system, the β-shifted peak was much larger than the graphitic peak, whereas in the nitrogen-implanted system, this ratio was reversed. This difference was related to the much higher electronegativity of the fluorine atom.

The last two columns of Table 3 contain the results of a quantitative analysis. They indicate a large loss of fluorine, in agreement with the qualitative analysis of the aforementioned spectra.

Table 3. Atomic Concentrations (atom %) in the Samples

	Theoretical	Pristine	Corrected	N^+-Implanted	F^+-Implanted
F	60.0	52.68	58.37	33.18	25.84
C	30.8	40.13	33.65	55.16	51.79
O	7.7	6.49	7.19	11.36	21.44
S	1.5	0.71	0.79	0.3	0.93

CONCLUSIONS

AM1 calculations with the charge–potential model correlate well with the C_{1s} core electron binding energies for a wide variety of polymers. The theoretical calculations provide a generally useful methodology for interpreting XPS spectra. The ion implantation of Nafion produces a carbonized surface layer. Analyses of XPS spectra provide a consistent assignment of the spectral components associated with the ion-implanted product.

The authors acknowledge funding by the U.S. Army Natick Soldier Center (DAAD 16-01-P-0389). They thank Thomas J. Tate for his assistance with ion implantation and Jack Hirsch for his help with the XPS measurements. F. E. Karasz also thanks Air Force Office of Scientific Research for additional support.

REFERENCES AND NOTES

1. Robertson, M. A. F.; Yeager, H. L. In Ionomers: Synthesis, Structure, Properties and Applications; Tant, M. R.; Mauritz, K. A.; Wilkes, G. L., Eds.; Chapman & Hall: London, 1997; p 290.
2. Hobson, L. J.; Ozu, H.; Yamaguchi, M.; Hayase, S. J Electrochem Soc 2001, 148, 1185.
3. Watanabe, M.; Uchida, H.; Igarashi, H. Macromol Symp 2000, 156, 223.
4. Walker, M.; Baumgartner, K. M.; Kaiser, M.; Kerres, J.; Ullrich, A.; Rauchle, E. J Appl Polym Sci 1999, 74, 67.
5. Carrette, L.; Friedrich, K. A.; Stimming, U. Chem Phys Chem 2000, 1, 162.
6. Wright, P. V. Electrochim Acta 1998, 43, 1137.
7. Nouel, K. M.; Fedkiw, P. S. Electrochim Acta 1998, 43, 2381.
8. Doyle, M.; Choi, S. K.; Proulx, G. J Electrochem Soc 2000, 147, 34.
9. Edmondson, C. A.; Stallworth, P. E.; Wintersgill, M. C.; Fontanella, J. J.; Dai, Y.; Greenbaum, S. G. Electrochim Acta 1998, 43, 1295.
10. Okada, T.; Moller-Holst, S.; Gorseth, O.; Kjelstrup, S. J Electroanal Chem 1998, 442, 137.
11. Okada, T.; Xie, G.; Gorseth, O.; Kjelstrup, S.; Nakamura, N.; Arimura, T. Electrochim Acta 1998, 43, 3741.
12. Zawodzinski, T. A.; Springer, T. E.; Uribe, F.; Gottesfeld, S. Solid State Ionics 1993, 60, 199.
13. Carrette, L.; Friedrich, K. A.; Stimming, U. Fuel Cells 2001, 1, 5.
14. Ren, X.; Springer, T. E.; Gottesfeld, S. J Electrochem Soc 2000, 147, 92.
15. Ren, X.; Springer, T. E.; Zawodzinski, T. A.; Gottesfeld, S. J Electrochem Soc 2000, 147, 466.
16. Ren, X.; Gottesfeld, S. J Electrochem Soc 2001, 148, 87.
17. Wagner, C. D.; Naumkin, A. V.; Kraut-Vass, A.; Allison, J. W.; Powell, C. J.; Rumble, J. R., Jr. NIST X-Ray Photoelectron Spectroscopy Database, version 3.2. http://srdata.nist.gov/xps, last accessed Feb. 1, 2003.
18. Beamson, G.; Briggs, D. High Resolution XPS of Organic Polymers—The Scienta ESCA300 Database; Wiley-Interscience: New York, 1992.
19. Pijpers, A. P.; Meier R. J Chem Soc Rev 1999, 28, 233.
20. Shulze, M.; Bolwin, K.; Gülzow, E.; Schnurnberger, W. Fresenius J Anal Chem 1995, 353, 778.
21. Shulze, M.; Lorenz, M.; Wagner, N.; Gülzow, E. Fresenius J Anal Chem 1999, 365, 106.
22. Siegbahn, K.; Nordling, C.; Johanson, G.; Hedman, J.; Hedén, P. F.; Hamrin, K.; Gelius, U.; Bergmark, T.; Werme, L. O.; Manne, R.; Baer, Y. ESCA Applied to Free Molecules; North Holland: Amsterdam, 1969; Chapter 5, pp 104–134.
23. Clark, D. T.; Feast, W. J.; Kilcast, D.; Musgrave, W. K. R. J Polym Sci Part A: Polym Chem 1973, 2, 389.
24. Endo, K.; Maeda, S.; Kaneda, Y. Polym J 1997, 29, 255.
25. Endo, K.; Maeda, S.; Aida, M. Polym J 1997, 29, 171.
26. Meier, R. J. J Electron Spectrosc Relat Phenom 1998, 94, 159.
27. Sleigh, C.; Pijpers, A. P.; Jaspers, A.; Coussens, B.; Meier, R. J. J Electron Spectrosc Relat Phenom 1996, 77, 41.
28. Susac, D.; Kono, M.; Wong, K. C.; Mitchell, K. A. R. Appl Surf Sci 2001, 174, 43.
29. Lee, Y.; Han, S.; Lim, H.; Jung, H.; Cho, J.; Kim, Y. J Adhes Sci Technol 2001, 15, 1079.
30. Popok, V. N.; Azarko, I. I.; Odzhaev, V. B.; Toth, A.; Khaibullin, R. I. Nucl Instrum Methods B 2001, 178, 305.
31. Dewar, M. J. S.; Zoebisch, E. G.; Healy, E. F.; Stewart, J. J. P. J Am Chem Soc 1985, 107, 3902.
32. Dewar, M. J. S.; Zoebisch, E. G. THEOCHEM 1988, 180, 1.
33. Dewar, M. J. S.; Yuan, Y. C. Inorg Chem 1990, 29, 3881.
34. Gould, G. L.; Eswara, V.; Trifu, R. M.; Castner, D. G. J Am Chem Soc 1999, 121, 3781.